

## Heavy-quarkonium hadron cross section in QCD at leading twist

François Arleo, Pol-Bernard Gossiaux, Thierry Gousset, and Jörg Aichelin

*SUBATECH, Laboratoire de Physique Subatomique et des Technologies Associées, UMR Université de Nantes, IN2P3/CNRS, Ecole des Mines de Nantes, 4, rue Alfred Kastler, 44070 Nantes cedex 03, France*

(Received 9 February 2001; published 29 November 2001)

We compute the total cross section of a heavy quarkonium on a hadron target in leading twist QCD, including target mass corrections. Our method relies on the analytical continuation of the operator product expansion of the scattering amplitude, obtained long ago by Bhanot and Peskin. The cross section has a simple partonic form, which allows us to investigate the phenomenology of  $J/\psi$  and  $Y$  dissociation by both pions and protons.

DOI: 10.1103/PhysRevD.65.014005

PACS number(s): 13.75.-n, 12.38.Bx, 13.85.Lg, 14.40.Gx

### I. INTRODUCTION

It has been conjectured that in ultrarelativistic collisions between heavy ions a quark gluon plasma (QGP) is formed for a very short period of time. Later it disintegrates into the hadrons which are finally seen in the detectors. It is the challenge of the present experiments at the CERN Super Proton Synchrotron (SPS) and at the BNL Relativistic Heavy Ion Collider (RHIC) to find observables which unambiguously signal the formation of the QGP.

One of the most promising suggestions advanced so far is the suppression of charmonium production in these collisions. It has been argued by Matsui and Satz [1] that the interaction between a heavy quark  $Q$  and antiquark  $\bar{Q}$  is screened in a QGP, and consequently the  $Q\bar{Q}$  bound pairs may not survive in this environment. The problem with this signal is that all other possible suppression mechanisms have to be well understood.

Whereas the general features of charmonium production in proton-proton collisions seem to be under control, already in proton-nucleus reactions the suppression is not well understood so far. Only recently, data have been published which show a different suppression of  $J/\psi$  and  $\psi'$  [2], and hence give the first hints that the  $J/\psi$  is formed inside the nucleus.

In heavy ion collisions the situation is even more difficult. There many particles are produced which possibly collide with a charmonium and may cause an observable suppression even if a QGP is not formed at all. In order to quantify such a suppression it is necessary to know the strength of these interactions. Experimentally the charmonium-hadron dissociation cross sections are not accessible. Therefore one has to rely on theoretical estimates. Three kinds of approaches have been advanced in the past.

The first approach is based on twist expansion techniques well known from deep inelastic scattering studies. It has been launched by Bhanot and Peskin [3,4] and was explicitly used in Ref. [4] for  $\psi$ - $p$  in the approximation of a vanishing proton mass. The whole approach gives a correct approximation of QCD provided that the heavy quark mass is large enough. It has thus the very advantage to be a well defined approximation scheme of the underlying theory. For realistic systems, such as charmonia and bottomonia, power correc-

tions are presumably non negligible, but some of them, namely finite target mass corrections, can be incorporated in a systematic way.

A second attempt is formulated within a constituent quark model. In an early study Martins *et al.* [5] have calculated a  $J/\psi$  dissociation cross section  $\sigma_{\psi\pi}$  by  $\pi$ 's of up to 7 mb at  $\sqrt{s}=4$  GeV, i.e., 0.8 GeV above  $m_{J/\psi}+m_{\pi}$ . This value has been reduced to about 1 mb for the same energy in a more recent study by Wong *et al.* [6] who used parameters adjusted to other elementary reactions.

A third approach is based on hadronic degrees of freedom. Invoking a local U(4) symmetry and employing pseudoscalar-pseudoscalar-vector coupling, Matinyan and Müller [7] investigated the dissociation of the  $J/\psi$  by exchange of a  $D$  or  $\bar{D}$  meson. Employing vector dominance to determine the coupling constants they arrive at  $\sigma_{\psi\pi} \approx 0.3$  mb for  $\sqrt{s}=4$  GeV. Later, Haglin [8] included four point interactions and a three vector-meson coupling and obtained a much larger cross section because the large suppression of the cross section due to the  $D$ -meson propagator is not present in the contact terms. Recently Lin and Ko [9] modified the details of this approach and included form factors. Depending on the form factor assumed they get  $\sigma_{\psi\pi}$  between 4 and 25 mb at  $\sqrt{s}=4$  GeV.

The purpose of this article is to extend the work of Ref. [4] in three different directions. First of all we include systematically the masses of the scattering partners using a method known from deep inelastic scattering studies. This allows for the calculation of the dissociation cross sections close to threshold where it is most relevant for the question at hand. Second the cross section of Ref. [4] is derived in a different, more direct fashion, again in analogy to the calculation of the forward Compton scattering amplitude in the operator product expansion. This cross section has a simple partonic expression, even when target mass corrections are included. We also explicitly derive how the reaction threshold is shifted by target mass corrections and how the cross section is modified in the vicinity of threshold. Third the calculation is extended towards other hadrons  $h$  and towards bottomonium which becomes an observable particle in the upcoming experiments at the RHIC and at the Large Hadron Collider (LHC) at CERN.

Target mass correction for  $J/\psi$ - $p$  cross section has been

examined in the framework of Bhanot and Peskin in Ref. [10]. These authors obtained their results in the form of sum rules. In principle these sum rules contain all of the above mentioned aspects but none is made explicit. Further we were neither capable to reproduce their exact expressions for the sum rules nor to find the trend they mention for the correction. We will clarify in the course of this study where we disagree.

## II. DERIVATION

In this section we generalize the expression obtained by Bhanot and Peskin [4] for the total cross section of a heavy quarkonium  $\Phi$  with a target hadron  $h$  by including finite target mass terms. The proposed analysis is close to that performed in the context of deep inelastic scattering [11,12].

### A. Short review of the framework

Let us first collect the material we need from Refs. [3,4]. We want to compute the  $\Phi$ - $h$  total cross section.<sup>1</sup> Our starting point is the expression for the forward  $\Phi$ - $h$  elastic scattering amplitude,  $\mathcal{M}_{\Phi h}$ . This amplitude depends on energy and it is convenient to express it in terms of

$$\lambda = \frac{(K+p)^2 - M^2 - m_h^2}{2M},$$

where  $K$  and  $p$  are the  $\Phi$  and  $h$  respective 4-momenta and  $M$  and  $m_h$  their respective masses. We note that  $\lambda$  is the hadron energy in the  $\Phi$  rest frame. Via the optical theorem, the forward scattering amplitude leads to the  $\Phi$ - $h$  total cross section

$$\sigma_{\Phi h}(\lambda) = \frac{1}{\sqrt{\lambda^2 - m_h^2}} \text{Im} \mathcal{M}_{\Phi h}(\lambda).$$

Notice that we use the same definition for  $\mathcal{M}$  as in Ref. [4].

In QCD, in the limit of a large heavy quark mass, the scattering amplitude has a twist expansion. In the  $\Phi$  rest frame the leading twist (LT) contribution is [4]

$$\mathcal{M}_{\Phi h}^{(\text{LT})}(\lambda) = a_0^3 \epsilon_0^2 \sum_{k \geq 1} d_{2k} \epsilon_0^{-2k} \langle h | F^{0\nu} (iD^0)^{2k-2} F_\nu^0 | h \rangle. \quad (1)$$

$a_0$  and  $\epsilon_0$  are, respectively, the Bohr radius and the Rydberg energy for the  $Q\bar{Q}$  system.

The above formula displays the factorization of the process in terms of hard coefficients  $d_n$  and soft matrix elements. Both should be evaluated at a factorization (and renormalization) scale  $\mu$ , to be chosen to minimize the influence of neglected higher order perturbative corrections. It is argued in Ref. [3] that  $\mu \sim \epsilon_0$ , though a precise determination fulfilling the latter requirement would need a complete

one-loop computation. In the phenomenological study, we will quantify the consequences of this scale uncertainty.

The coefficients  $d_n$  correspond to matrix elements of definite operators evaluated in the  $\Phi$  state. These are computable in perturbative QCD and have been made explicit in Ref. [3] for 1S and 2S  $\Phi$  states to leading order in the coupling and to leading order in  $1/N_c$ , where  $N_c$  is the number of colors. For 1S state<sup>2</sup> they read

$$d_n = \frac{16^3}{3N_c^2} B(n+5/2, 5/2),$$

where  $B(\mu, \nu)$  is the Euler beta function. For later convenience we remark that  $d_n$  can be expressed as the  $n$ -th moment of a given function  $f$  through

$$d_n = \int_0^1 \frac{dx}{x} x^n f(x),$$

with

$$f(x) = \frac{16^3}{3N_c^2} x^{5/2} (1-x)^{3/2}.$$

For every  $k$  in Eq. (1) a gluon twist-2 operator evaluated in the hadron  $h$  (*spin-averaged*) state also appears. Each of these matrix elements is a traceless fully symmetric rank  $2k$  tensor built from the hadron momentum  $p^\mu$ . It turns out that a tensor having these properties is necessarily proportional to [11]

$$\Pi^{\mu_1 \dots \mu_{2k}}(p) = \sum_{j=0}^k (-m_h^2)^j \frac{(2k-j)!}{2^j (2k)!}$$

$$\times \left[ \sum_{\text{perm.}} \underbrace{g \otimes \dots \otimes g}_j \otimes \underbrace{p \otimes \dots \otimes p}_{2k-2j} \right]^{\mu_1 \dots \mu_{2k}},$$

where the tensor in the  $j$ th term on the right-hand side is the sum of the  $(2k)!/[2^j j! (2k-2j)!]$  distinct tensors one can construct by multiplying  $j$   $g^{\nu\rho}$ 's and  $(2k-2j)$   $p^\sigma$ 's. The matrix element needed in Eq. (1) is therefore proportional to  $\Pi^{0 \dots 0}(p)$  and writes

$$\begin{aligned} & \langle h(p) | F^{0\nu} (iD^0)^{2k-2} F_\nu^0 | h(p) \rangle \\ &= A_{2k} \Pi^{0 \dots 0}(p) \\ &= A_{2k} \sum_{j=0}^k \frac{(2k-j)!}{j! (2k-2j)!} (-m_h^2/4)^j \lambda^{2k-2j}. \end{aligned} \quad (2)$$

<sup>1</sup>Throughout this paper we restrict ourselves to *spin-averaged* cross sections without further mention.

<sup>2</sup>The present consideration applies to 2S state as well but is left out until Appendix B.

This set of matrix elements is related to the unpolarized gluon density  $G$  in the hadron target. One can see this from the matrix element definition of  $G$ , see, e.g., [13], which in the light cone gauge  $A^+ = 0$  reads

$$xG(x) = \frac{1}{p^+} \int \frac{dy^-}{2\pi} e^{ixp^+y^-} \langle h(p) | F^{+\nu}(0) F_{\nu^+}(y^-) | h(p) \rangle.$$

In the parton model the argument of  $G$ , i.e.,  $x$ , is interpreted as the fraction of the hadron light cone momentum  $p^+$  carried by the gluon. Taking the  $n$ th moment of  $G(x)$ , we get

$$\int_0^1 \frac{dx}{x} x^n G(x) = \frac{1}{(p^+)^n} \langle h(p) | F^{+\nu} (i\partial^+)^{n-2} F_{\nu^+} | h(p) \rangle.$$

Since  $D^+ = \partial^+$  in the  $A^+ = 0$  gauge we recognize

$$\begin{aligned} \langle h(p) | F^{+\nu} (iD^+)^{2k-2} F_{\nu^+} | h(p) \rangle &= A_{2k} \Pi^{+\cdots+}(p) \\ &= A_{2k} (p^+)^{2k}, \end{aligned}$$

i.e.,

$$A_n = \int_0^1 \frac{dx}{x} x^n G(x).$$

### B. Massless target

In the present subsection we want to illustrate the general method in the case of vanishing target mass,  $m_h = 0$ . Then Eq. (2) simplifies to

$$\langle h | F^{0\nu} (iD^0)^{2k-2} F_{\nu^0} | h \rangle = A_{2k} \lambda^{2k},$$

and Eq. (1) thus becomes

$$\mathcal{M}_{\Phi h}^{(\text{LT})}(\lambda) = a_0^3 \epsilon_0^2 \sum_{k \geq 1} d_{2k} A_{2k} (\lambda / \epsilon_0)^{2k}. \quad (3)$$

It is useful to study the scattering amplitude  $\mathcal{M}_{\Phi h}$  throughout the complex plane of the energy. To avoid confusion, we will from now on reserve the notation  $\lambda$  to real values and define  $\underline{\lambda}$  as the extension of  $\lambda$  to complex values. Using the d'Alembert criterion one easily checks that the convergence radius of the power series (3), now considered with the complex argument  $\underline{\lambda}$ , is equal to  $\epsilon_0$ . As extensively discussed in Ref. [4], the twist expansion of the scattering amplitude provides an expression for  $\mathcal{M}_{\Phi h}^{(\text{LT})}(\lambda)$  in the *unphysical* region of energies. Since we are interested in *physical* energies we have to perform an analytic continuation of the power series.

Before doing so let us first elaborate on possible differences between  $\mathcal{M}_{\Phi h}^{(\text{LT})}$  and the *full* scattering amplitude  $\mathcal{M}_{\Phi h}$ , i.e., including higher twist terms. It turns out from the analysis below that the singularities (branch points) of  $\mathcal{M}_{\Phi h}^{(\text{LT})}$  on the boundary of the convergence disk of the power series lie at  $\underline{\lambda} = \pm \epsilon_0$ . This is not what is expected for the locations of the (first) branch points of  $\mathcal{M}_{\Phi h}$ , i.e., the locations of the thresholds for both reactions  $\Phi + h \rightarrow X$  and  $\Phi$

$+ \bar{h} \rightarrow X$ , which are  $\underline{\lambda} = \pm m_h$ . The technical reason for the difference is, of course, that  $m_h$  occurs nowhere in Eq. (3). In the twist expansion approach the locations of the singularities of the full scattering amplitude may be affected by higher twist corrections. We verify that this is the case for the above reactions by taking into account elastic unitarity corrections for which the thresholds are clearly located at  $\underline{\lambda} = \pm m_h$ .<sup>3</sup> In the next section we shall see how  $m_h \neq 0$  corrections affect the locations of the LT reaction thresholds.

Since the convergence radius of the power series (3) is nonzero the LT amplitude<sup>4</sup> can be unambiguously determined throughout the  $\underline{\lambda}$  complex plane from the sole knowledge of Eq. (3), using the Mellin transform machinery. We first remark that  $M_n = d_n A_n$  being a product of moments one can express

$$M_n = \int_0^1 \frac{dx}{x} x^n h(x), \quad (4)$$

with

$$h(x) = G \otimes f(x),$$

and the convolution product defined as

$$G \otimes f(x) = \int_x^1 \frac{dy}{y} G(y) f(x/y).$$

Now, plugging Eq. (4) in Eq. (3) for  $|\underline{\lambda}| < \epsilon_0$ , freely interchanging summation with integration and summing the ensuing geometrical series, one finds

$$\mathcal{M}(\underline{\lambda}) = a_0^3 \epsilon_0^2 \int_0^1 \frac{dx}{x} h(x) \frac{x^2 (\underline{\lambda} / \epsilon_0)^2}{1 - x^2 (\underline{\lambda} / \epsilon_0)^2}.$$

The key point is that this integral representation can be extended throughout the entire complex plane except for the two branch points  $\underline{\lambda} = \pm \epsilon_0$ . The analytic continuation of Eq. (3) to energies  $\lambda > \epsilon_0$  is then easily derived

$$\mathcal{M}(\underline{\lambda} = \lambda \pm i\varepsilon) = a_0^3 \epsilon_0^2 \int_0^1 dx h(x) \frac{x (\lambda / \epsilon_0)^2}{1 - x^2 (\lambda / \epsilon_0)^2 \mp i\varepsilon}, \quad (5)$$

and its imaginary part given by

$$\text{Im} \mathcal{M}(\lambda) = \frac{1}{2i} [\mathcal{M}(\lambda + i\varepsilon) - \mathcal{M}(\lambda - i\varepsilon)] = \frac{\pi}{2} a_0^3 \epsilon_0^2 h(\epsilon_0 / \lambda).$$

Putting all things together, one gets

<sup>3</sup>Let us note in passing one important phenomenological consequence of the LT analysis: what we call the *total* (LT) cross section does not in fact include processes such as the elastic one. The word “total” is thus misleading, at least in the threshold region.

<sup>4</sup>From now on  $\mathcal{M}$  always refers to the leading twist part of the forward  $\Phi$ - $h$  elastic scattering amplitude and we drop the indices (LT) and  $\Phi h$  for simplicity.

$$\text{Im}\mathcal{M}(\lambda) = \frac{\pi\lambda}{2} a_0^3 \epsilon_0 \frac{16^3}{3N_c^2} \int_{\epsilon_0/\lambda}^1 dx G(x) \frac{(x\lambda/\epsilon_0 - 1)^{3/2}}{(x\lambda/\epsilon_0)^5}. \quad (6)$$

Dividing Eq. (6) by  $\lambda$  (the flux factor when  $m_h=0$ ) we recover the partonic expression of the  $\Phi$ - $h$  total cross section as obtained by Bhanot and Peskin within a parton model approach, i.e.,

$$\sigma_{\Phi h}(\lambda) = \int_0^1 dx G(x) \sigma_{\Phi g}(x\lambda), \quad (7)$$

with the  $\Phi$ -gluon cross section

$$\sigma_{\Phi g}(\omega) = \frac{16^3 \pi}{6N_c^2} a_0^3 \epsilon_0 \frac{(\omega/\epsilon_0 - 1)^{3/2}}{(\omega/\epsilon_0)^5} \theta(\omega - \epsilon_0), \quad (8)$$

$\omega$  corresponding to the gluon energy in the  $\Phi$  rest frame. Aside from its energy dependence, the  $\Phi$ -gluon cross section is driven by  $a_0^3 \epsilon_0 \propto \alpha_S a_0^2$ , as expected in QCD for the interaction of a small color singlet dipole of size  $a_0$ .

In this formulation one important physical aspect is made transparent [3,4]: the leading twist analysis describes the  $\Phi$  dissociation by gluons into a  $Q$  and a  $\bar{Q}$

$$\Phi + g \rightarrow Q + \bar{Q}.$$

To be energetically possible the gluon energy has therefore to be larger than the  $Q\bar{Q}$  Coulomb binding energy  $\epsilon_0$ . In view of the fact that the confinement scale is small as compared to  $\epsilon_0$  the LT analysis then provides a description of  $\Phi$  dissociation into open channels, e.g.,  $Q\bar{q} + \bar{Q}q$ . Let us emphasize that this dissociation is precisely the process of interest for the question of  $\Phi$  suppression in heavy ion collisions.

An important aspect for the phenomenology of the above cross section is its limiting behaviors for both small and large energy regimes. These are linked to the  $x \rightarrow 1$  and  $x \rightarrow 0$  behaviors of  $G$ , respectively. It is then convenient to have in mind the simple, yet standard, parametrization

$$G(x) = A (1-x)^{\eta/x^{1+\delta}}. \quad (9)$$

With this ansatz one can write down exact asymptotic formulas either by following the reasoning of Ref. [4] or by noticing that the  $\Phi$ - $h$  cross section is proportional to a hypergeometric function. This is most easily done by changing variable  $x$  to  $t = (x\lambda/\epsilon_0 - 1)/(\lambda/\epsilon_0 - 1)$  in Eq. (6). Then one recognizes [14]

$$\begin{aligned} \sigma(\lambda) &= \frac{16^3 \pi}{6N_c^2} a_0^3 \epsilon_0 A B(\eta + 1, 5/2) (\lambda/\epsilon_0 - 1)^{\eta+5/2} \\ &\times (\lambda/\epsilon_0)^{\delta-} {}_2F_1\left(\delta + 6, 5/2; \eta + 7/2; 1 - \lambda/\epsilon_0\right). \end{aligned}$$

For  $\lambda$  in the neighborhood of  $\epsilon_0$ , i.e., the  $m_h=0$  threshold, the hypergeometric function approaches 1 and we get

$$\sigma_{\Phi h}(\lambda) \sim \frac{16^3 \pi}{6N_c^2} a_0^3 \epsilon_0 A B(\eta + 1, 5/2) (\lambda/\epsilon_0 - 1)^{\eta+5/2}. \quad (10)$$

For large energies, using

$${}_2F_1\left(\delta + 6, \frac{5}{2}; \eta + \frac{7}{2}; 1 - \lambda/\epsilon_0\right) \sim \frac{B(\delta + 7/2, 5/2)}{B(\eta + 1, 5/2)} (\lambda/\epsilon_0)^{-5/2},$$

one obtains

$$\sigma_{\Phi h}(\lambda) \sim \frac{16^3 \pi}{6N_c^2} a_0^3 \epsilon_0 A B(\delta + 7/2, 5/2) \left(\frac{\lambda}{\epsilon_0}\right)^{\delta}. \quad (11)$$

The high energy cross section is primarily geometrical (remember  $a_0^3 \epsilon_0 \propto \alpha_S a_0^2$ ). In addition to this simple behavior, there is a nontrivial energy dependence coming from the small  $x$  behavior of the gluon density.

For phenomenological investigations we shall also use slightly more involved forms for  $G(x)$  as obtained in parton distribution function studies. In this case the connection to  ${}_2F_1$  is lost. One may, however, derive similar asymptotic expressions by first expanding the gluon distribution either in the neighborhood of 1 or 0.

### C. Massive target

Having illustrated the method for the case  $m_h=0$ , we now turn to the general case  $m_h \neq 0$ . Plugging Eq. (2) into Eq. (1) leads to

$$\begin{aligned} \mathcal{M}'(\lambda) &= a_0^3 \epsilon_0^2 \sum_{k \geq 1} M_{2k} \sum_{j=0}^k \frac{(2k-j)!}{j!(2k-2j)!} (\lambda/\epsilon_0)^{2k-2j} \\ &\times \left(-\frac{m_h^2}{4\epsilon_0^2}\right)^j, \end{aligned}$$

with  $M_{2k} = d_{2k} A_{2k}$ . We thus get an amplitude which may be considered as a double power series in  $\lambda$  and  $m_h$ . The study of this double series with complex arguments  $\lambda \rightarrow \underline{\lambda}$  and  $m_h^2/(4\epsilon_0^2) \rightarrow z$  shows that it is absolutely convergent for  $|\underline{\lambda}/\epsilon_0| + |z| < 1$ . In this domain, defining  $k' = k - j$  we may rewrite the series as

$$\begin{aligned} \mathcal{M}'(\lambda, m_h) &= a_0^3 \epsilon_0^2 \sum_{j \geq 0, k' \geq 1} (\lambda/\epsilon_0)^{2k'} M_{2(k'+j)} \frac{(2k'+j)!}{j!(2k')!} \\ &\times \left(-\frac{m_h^2}{4\epsilon_0^2}\right)^j + a_0^3 \epsilon_0^2 \sum_{j \geq 1} M_{2j} \left(-\frac{m_h^2}{4\epsilon_0^2}\right)^j. \quad (12) \end{aligned}$$

The second term on the right-hand side corresponds to the power-series expansion of the scattering amplitude  $\mathcal{M}$  of Sec. II B evaluated at the complex plane location  $\underline{\lambda} = im_h/2$ :

$$a_0^3 \epsilon_0^2 \sum_{j \geq 1} M_{2j} \left(-\frac{m_h^2}{4\epsilon_0^2}\right)^j = \mathcal{M}(im_h/2).$$



From the representation (5) of the scattering amplitude we immediately see that  $\mathcal{M}(im_h/2)$  is well defined and real for every (real)  $m_h$ . We thus ignore this term in the following since it does not contribute to the total cross section at leading twist.

Let us now concentrate on the first term on the right-hand side of Eq. (12). We use the same reasoning as in Sec. II B considering now the double series (12) with complex arguments  $\underline{\lambda}$  and  $z$  instead of  $\lambda$  and  $m_h^2/(4\epsilon_0^2)$ . Expressing first  $M_n$  as the  $n$ -th moment of  $h = G \otimes f$  one can write

$$M_{2(k'+j)} \frac{(2k'+j)!}{j!(2k')!} (-z)^j = \int_0^1 dx x^{2k'} h(x) \frac{(2k'+j)!}{j!(2k')!} \times (-x^2 z)^j.$$

In the convergence domain of the double series, the series in  $j$  may be summed up. Introducing

$$M'_n(z) = \sum_{j \geq 0} M_{n+2j} \frac{(n+j)!}{j!n!} (-z)^j = \int_0^1 dx x^n h(x) \frac{1}{(1+x^2 z)^{n+1}}, \quad (13)$$

we may then follow another time the reasoning of Sec. II B replacing  $M_n$ , Eq. (4), by  $M'_n(z)$  as given by Eq. (13). We notice in passing that the modified moments  $M'_n(z)$  are analytic functions of  $z$  throughout the complex plane except at  $z = -1$ .

For simplicity we restrict ourselves to physical masses, i.e., to the positive real axis of  $z$  where the above integral representation is well defined. Then, two cases show up depending on whether  $m_h < 2\epsilon_0$  or not. The former case is the one relevant to phenomenology but we consider both cases in turn for completeness.

For  $m_h < 2\epsilon_0$ , we restore  $z = m_h^2/(4\epsilon_0^2)$  and change the variable to  $x' = x/(1+x^2 m_h^2/(4\epsilon_0^2))$ . Then we have

$$M'_n \left( \frac{m_h^2}{4\epsilon_0^2} \right) = \int_0^{[1+m_h^2/(4\epsilon_0^2)]^{-1}} dx' x'^n \frac{h(x)}{1-x^2 m_h^2/(4\epsilon_0^2)},$$

with  $x$  understood as a function of  $x'$ . In this form we can easily follow the reasoning of Sec. II B because the integration range does not play a role until one cuts the amplitude. This cutting imposes  $x' = \epsilon_0/\lambda$  and thus results in a non-vanishing imaginary part for  $\lambda > \lambda_0 = \epsilon_0 + m_h^2/(4\epsilon_0)$ . Above this threshold

$$\begin{aligned} \text{Im} \mathcal{M}'(\lambda) &= \frac{\pi}{2} a_0^3 \epsilon_0^2 \frac{h(\epsilon_0/\lambda_+)}{1 - m_h^2/(4\lambda_+^2)} \\ &= \frac{\pi}{2} a_0^3 \epsilon_0^2 \frac{\lambda_+}{\sqrt{\lambda^2 - m_h^2}} h(\epsilon_0/\lambda_+), \end{aligned} \quad (14)$$

where  $\lambda_+ = (\lambda + \sqrt{\lambda^2 - m_h^2})/2$ . Dividing Eq. (14) by the flux factor we obtain for the total cross section

$$\sigma_{\Phi h}(\lambda) = \frac{\lambda_+^2}{\lambda^2 - m_h^2} \int_0^1 dx G(x) \sigma_{\Phi g}(x\lambda_+). \quad (15)$$

Some comments are in order. We first stress that, as in the  $m_h = 0$  case, one arrives at a simple partonic form of the cross section. This means, in particular, that the physical discussion we gave after Eq. (7), based on the subprocess  $\Phi + g \rightarrow Q + \bar{Q}$ , still holds in the massive target case. Apart from the prefactor, the only modification between Eq. (15) and Eq. (7) is the modification of the expression for the gluon energy in the partonic cross section  $\sigma_{\Phi g}$ . The change from  $x\lambda$  to  $x\lambda_+$  may be given a heuristic interpretation in the parton context using light cone coordinates.<sup>5</sup> In the  $\Phi$  rest frame let us choose the third axis along the hadron  $h$  momentum and form  $p^+ = (\lambda + \sqrt{\lambda^2 - m_h^2})/\sqrt{2}$  and  $p^- = m_h^2/(2p^+)$ . In the parton picture the gluon causing the dissociation is picked up from the hadron  $h$  and has a negligible transverse momentum, and hence a negligible minus momentum. Its energy is then easily expressed in terms of  $x$ , the light cone (plus) momentum fraction of the gluon, and reads  $\omega = xp^+/\sqrt{2}$ , i.e.,  $\omega = x\lambda_+$ .

Our understanding of the prefactor is more formal. We observe that Eq. (14) may be rewritten as

$$\text{Im} \mathcal{M}'(\lambda) d\lambda = \text{Im} \mathcal{M}(\lambda_+) d\lambda_+,$$

a relation which entails the (formal) identity

$$M'_{-1}(z) = M_{-1}, \quad \forall z, \quad (16)$$

which can also be obtained from a direct comparison between Eqs. (13) and (4).

Next, we point out that, as expected, the  $m_h \neq 0$  corrections are sizeable only for small energies. The first aspect of these corrections is that, as above mentioned, the threshold is now located at

$$\lambda_0 = \epsilon_0 + \frac{m_h^2}{4\epsilon_0}. \quad (17)$$

As in the massless case this corresponds to the need to find in  $h$  a gluon with an energy  $\omega \geq \epsilon_0$  sufficient to dissociate the  $\Phi$ . With  $\omega = x\lambda_+$  and  $x \leq 1$  this gives a  $\lambda_+$  threshold  $\lambda_{+0} = \epsilon_0$ , leading to Eq. (17). The second aspect is that the cross section behavior for  $\lambda \rightarrow \lambda_0$  is given by Eq. (10) with an argument  $\lambda_+$  instead of  $\lambda$  and a prefactor

$$\frac{\lambda_+^2}{\lambda^2 - m_h^2} \sim \left( \frac{\epsilon_0}{\epsilon_0 - m_h^2/(4\epsilon_0)} \right)^2.$$

Let us now investigate the  $m_h > 2\epsilon_0$  case. One may perform the same change of variable in the intervals  $[0, 2\epsilon_0/m_h]$  and  $[2\epsilon_0/m_h, 1]$  leading to

<sup>5</sup>Such a connection between light cone variables and  $m_h \neq 0$  correction is discussed for deep inelastic scattering in [15].

$$M'_{n'}(m_h^2/(4\epsilon_0^2)) = \int_0^{\epsilon_0/m_h} \frac{dx'}{x'} x'^{n'} \frac{h(x)}{1-x^2 m_h^2/(4\epsilon_0^2)} \\ + \int_{[1+m_h^2/(4\epsilon_0^2)]^{-1}}^{\epsilon_0/m_h} \frac{dx'}{x'} x'^{n'} \frac{h(x)}{x^2 m_h^2/(4\epsilon_0^2) - 1}.$$

The threshold becomes  $\lambda_0 = m_h$  and one finds

$$\text{Im}\mathcal{M}'(\lambda) = \frac{\pi}{2} a_0^3 \epsilon_0^2 \left( \frac{h(\epsilon_0/\lambda_+)}{1 - m_h^2/4\lambda_+^2} + \frac{h(\epsilon_0/\lambda_-)}{m_h^2/4\lambda_-^2 - 1} \right), \quad (18)$$

with  $\lambda_{\pm} = (\lambda \pm \sqrt{\lambda^2 - m_h^2})/2$ . We notice that the first contribution is the one already obtained in the case  $m_h < 2\epsilon_0$ . The second term is new but contributes only in the range  $m_h \leq \lambda \leq \epsilon_0 + m_h^2/(4\epsilon_0)$ . We further point out that the relevant energy variable is now half the difference between energy and momenta, instead of half the sum for the first term, and that the present result Eq. (18) is again consistent with the  $M_{-1}$  sum rule (16). Finally, in the neighborhood of threshold the cross section now amounts to

$$\sigma_{\Phi h}(\lambda) \sim \frac{1}{2(\lambda^2/m_h^2 - 1)} \frac{\pi}{2} a_0^3 \epsilon_0 \frac{h(2\epsilon_0/m_h)}{m_h/2\epsilon_0}. \quad (19)$$

### III. PHENOMENOLOGY

#### A. Choice of parameters

In view to give numerical values for  $\Phi$ - $h$  leading twist total cross sections and thresholds, it is necessary to fix, on the one hand, the heavy quark mass  $m_Q$  and the quarkonium Rydberg energy  $\epsilon_0$ , and, on the other hand, the gluon density in the target.

##### 1. Quarkonium sector

The above described QCD analysis assumes that the  $Q\bar{Q}$  binding potential is well approximated by the Coulomb part of the QCD potential [3]. Treating the 1S and 2S heavy quarkonia as Coulombic states leads to

$$M_{Q\bar{Q}}(1S) = 2m_Q - \epsilon_0, \quad (20)$$

$$M_{Q\bar{Q}}(2S) = 2m_Q - \frac{\epsilon_0}{4}, \quad (21)$$

that is

$$m_Q = \frac{1}{6} [4 M_{Q\bar{Q}}(2S) - M_{Q\bar{Q}}(1S)],$$

$$\epsilon_0 = \frac{4}{3} [M_{Q\bar{Q}}(2S) - M_{Q\bar{Q}}(1S)].$$

This gives for charm and bottom respectively [set (i)]

$$\epsilon_{0c} = 0.78 \text{ GeV}, \quad m_c = 1.94 \text{ GeV},$$

$$\epsilon_{0b} = 0.75 \text{ GeV}, \quad m_b = 5.10 \text{ GeV}.$$

One way of estimating the applicability of the heavy quark analysis to charmonia and bottomonia is to compare the size of each Coulomb-state to typical confining distances. One may first evaluate the Bohr radius  $a_0 = 1/\sqrt{\epsilon_0 m_Q}$ , this gives  $a_{0c} = 0.16$  fm for charm and  $a_{0b} = 0.10$  fm for bottom. Recalling that the 1S-state root mean square is given by  $r(1S) = \sqrt{3} a_0$  one finds that the 1S-state size remains somewhat below typical confining distances. We then consider that the LT analysis may be at least indicative of the behavior of 1S-state cross section. Computing the size of 2S-states with  $r(2S) = \sqrt{30} a_0$ , one sees that the situation is much less favorable for 2S-states, especially for charmonium. The application of the framework to  $Y'$  is given in Appendix B.

In addition to the question of the validity of the computation of 2S-state cross section within the LT analysis this also led us to reconsider the above choice of parameters. For this we drop Eq. (20) and propose to fix the Rydberg energy to the energy gap between the 1S state and the open flavor production. With Eq. (21) this is equivalent to putting  $m_c = m_D$  for charm and  $m_b = m_B$  for bottom. We then have the alternative set [set (ii)]

$$\epsilon_{0c} = 0.62 \text{ GeV}, \quad m_c = 1.86 \text{ GeV},$$

$$\epsilon_{0b} = 1.10 \text{ GeV}, \quad m_b = 5.28 \text{ GeV}.$$

As we shall see, the cross section is only sizeable at large energy. In this region the magnitude of the cross section is driven by the factor  $a_0^3 \epsilon_0 = 1/\sqrt{m_Q^3 \epsilon_0}$  [see Eq. (11)]. Taking set (ii) instead of set (i) results in a 20% cross section increase for charm and in a 22% cross section decrease for bottom. It turns out that this uncertainty is smaller than the one coming from scale fixing discussed in the next section. We will therefore limit our further considerations to cross sections obtained using set (i).

##### 2. Gluon distributions

The other important input for the computation is the gluon density  $G_h$  in the hadron  $h$  considered. At this point one should remember that this density depends on the factorization scale  $\mu$  [see paragraph following Eq. (1)]. In the  $\Phi$ - $h$  cross section, not only  $G_h$  is a function of  $\mu$ , but also  $\sigma_{\Phi g}$ . Part of the dependence stands in the explicit coupling of the gluon with the  $\Phi$  constituents, corresponding to the factor  $\alpha_S$  in  $a_0^3 \epsilon_0 \propto \alpha_S a_0^2$ , though the knowledge of the full dependence requires a complete one-loop calculation. Lacking such an analysis led us first to restrict ourselves to the so-called leading order (LO) gluon distributions (i.e., their evolutions are computed to one-loop) and correspondingly to the LO running coupling. Second, we investigated with some care the variation of our results with the choice of different factorization scales.

We started this analysis with the prescription suggested in Ref. [3] that  $\mu \sim \epsilon_0$ . For such a low scale the only available parametrization for the proton is the Glück-Reya-Vogt [16], (GRV94) leading order (LO) parametrization.<sup>6</sup> These authors have proposed a parametrization for the pion too [17]. Concerning the  $x$  dependence of the various gluon densities, one should notice that the intermediate- $x$  region is rather well monitored, while the small- $x$  region is poorly understood, especially for the pion case. Thanks to the DESY  $ep$  collider HERA measurements the situation for the proton is much better. Including these data Glück-Reya-Vogt have provided a new parametrization [18] but its lower scale is larger than that needed for this study. However we checked that at a scale large enough for both to be compared the difference between the gluon distribution of Ref. [18] and that of Ref. [16] is not significant.

We also examined, at a larger factorization scale, the consequences of different parametrizations of the gluon distribution in the proton, considering in turn 1998 Martin-Roberts-Stirling-Thorne (MRST98) LO [19] and CTEQ5L [20].

### B. Cross section variation with energy including target mass corrections

As we shall see in the next section, the cross section at a given energy depends on the choice of parameters. Its general trend, however, is rather independent of a specific choice. We therefore begin our phenomenological study by discussing in this section those aspects that only weakly depend on the quarkonium parameters and gluon distributions.

In Sec. II we have seen that one can distinguish two extreme energy regimes in the  $\Phi$ - $h$  cross section: a threshold region and a high energy regime. The high-energy cross section is independent of the target mass and is given by

$$\sigma(\lambda) \sim \sigma_{\text{as}}(\lambda) = C (\lambda/\epsilon_0)^\delta$$

for gluon densities  $G(x) \sim \text{const.}/x^{1+\delta}$  at small  $x$ . The constant  $C$  depends on details of the gluon density and on the parameters describing the charmonium sector [see, e.g., Eq. (11)]. In every case discussed in Sec. III A the relative difference between this asymptotic cross section  $\sigma_{\text{as}}$  and the full result is less than 25% for  $\lambda > 30 \epsilon_0$ . For  $J/\psi$  this translates roughly into  $\sqrt{s} > 13$  GeV and for  $\Upsilon$  into  $\sqrt{s} > 23$  GeV.

For  $m_h = 0$  the cross section is very small in the threshold region. We found that it is less than 10% of  $\sigma_{\text{as}}$  for  $\lambda < 2-3 \epsilon_0$ , i.e.,  $\sqrt{s} < 5$  GeV for  $J/\psi$  and 12 GeV for  $\Upsilon$ .

Let us now investigate the effect of a finite  $m_h$ . Figure 1 shows the ratio of  $\sigma_{\Phi h}(\lambda, m_h)$  and  $\sigma_{\Phi h}(\lambda, 0)$  for two hypothetical hadron masses such that  $m_h < 2 \epsilon_0$ , namely  $m_h = \epsilon_0/5$  (“pion-like,” *dotted*) and  $m_h = \epsilon_0$ . The latter case has been computed for a pion gluon distribution (“rho-like,” *dashed*) as well as for a proton gluon distribution (“proton-

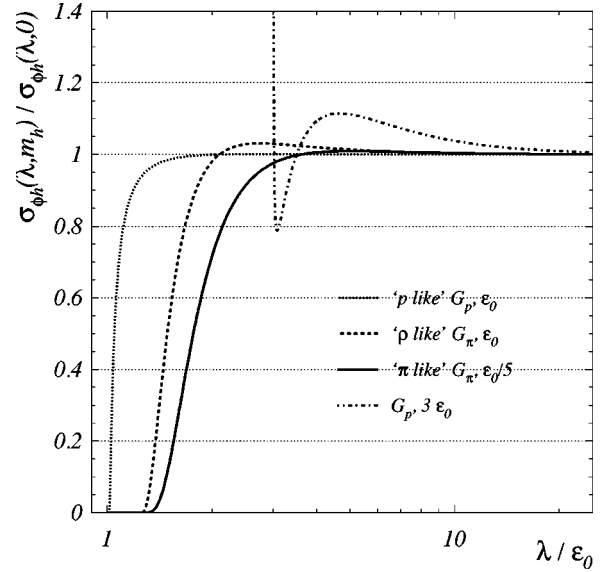


FIG. 1. Ratio of the corrected [ $\sigma_{\Phi h}(\lambda, m_h)$ ] over the uncorrected [ $\sigma_{\Phi h}(\lambda, 0)$ ] cross sections as a function of  $\lambda/\epsilon_0$ . Calculations are performed for hadron masses  $m_h = \epsilon_0/5$ ,  $\epsilon_0$  and  $m_h = \epsilon_0$ ,  $3\epsilon_0$  using the gluon density  $G_h(x, \mu = 0.75 \text{ GeV})$  in the pion [17] and in the proton [16], respectively (see text).

like,” *solid*). This ratio is plotted as a function of  $\lambda/\epsilon_0$  and is then identical for charm and bottom mesons.

In addition to the shift of the threshold Eq. (17), we observe that the inclusion of finite mass correction reduces the cross section close to threshold. This result is opposite to what is found in Ref. [10],<sup>7</sup> where it is argued that the target mass correction tends to increase the  $J/\psi$ - $p$  cross section near threshold. We notice that the mass correction is important only for  $\lambda < 2-3 \epsilon_0$ . This implies that it is of limited phenomenological interest since, as we have seen above, the cross section is very small in this low energy region.

In Sec. II C we identified a different behavior in the case of heavy targets ( $m_h > 2 \epsilon_0$ ). Figure 1 shows mass correction for a hadron with mass  $m_h = 3 \epsilon_0$  and a gluon distribution  $G_p$  given by Ref. [16] (*dash-dotted*). The cross section diverges at threshold ( $\lambda/\epsilon_0 = m_h/\epsilon_0 = 3$ ), as can be seen in Eq. (19). The window for which the cross section gets sizeable is very narrow, however. Thus this threshold behavior has probably very little phenomenological implications.

## C. $\Phi$ - $h$ absolute cross sections

### 1. Factorization scale dependence

Before addressing in the next section the magnitude of the cross sections, the influence of the factorization scale is quantitatively investigated. More specifically the three choices:  $\mu^2 = \epsilon_0^2$ ,  $2\epsilon_0^2$ , and  $4\epsilon_0^2$  were considered.

We made this investigation for the bottom channel with the parameter set (i). In addition to the heavy quark mass,

<sup>6</sup>It should be borne in mind that at such a low normalization scale the gluon distribution is less constrained by experimental data than by model assumptions.

<sup>7</sup>We give ample details on the comparison between the present approach and that of Ref. [10] in Appendix A.

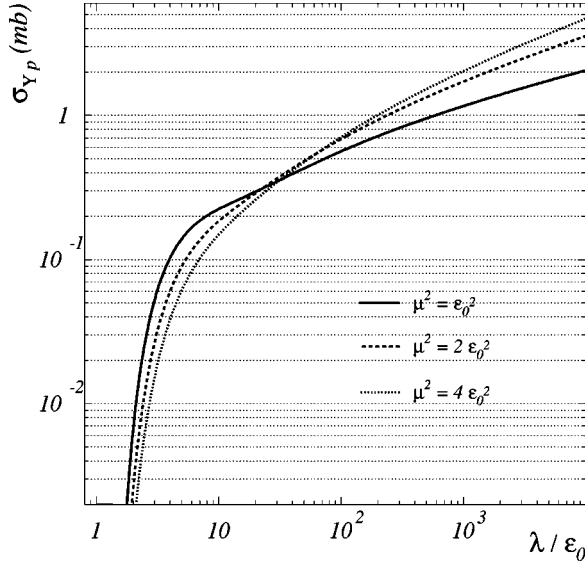


FIG. 2. Absolute  $\sigma_{Yp}^{(\mu^2)}$  cross section as a function of  $\lambda/\epsilon_0$  for different factorization scale:  $\mu^2 = \epsilon_0^2$  (solid),  $\mu^2 = 2\epsilon_0^2$  (dashed), and  $\mu^2 = 4\epsilon_0^2$  (dotted). The gluon distribution used is GRV94 LO.

this choice benefits from the numerical coincidence that<sup>8</sup>

$$a_{0b}\epsilon_{0b} = \sqrt{\frac{\epsilon_{0b}}{m_b}} \approx \frac{2}{3} \alpha_S(\mu^2 = \epsilon_{0b}^2),$$

as expected for a large enough  $\epsilon_0$  if the factorization scale is  $\mu^2 = \epsilon_0^2$ .

Let us first define the  $Y$ - $p$  cross section,  $\sigma_{Yp}^{(\mu^2 = \epsilon_0^2)}$ , computed with the prescription  $\mu^2 = \epsilon_0^2$ , to be that given by Eq. (7) with the parameter set (i) for the bottomonium and the proton distribution GRV94 LO evaluated at  $\mu^2 = \epsilon_0^2$ . We next define  $\sigma_{Yp}^{(\mu^2)}$  at another scale to be that computed with GRV94 LO evaluated at  $\mu^2$  and multiplied by the factor

$$\alpha_S(\mu^2)/\alpha_S(\epsilon_0^2),$$

which takes into account the change of the coupling of the gluon to the  $\Phi$  constituents, and decreases down to 63% for  $\mu^2 = 4\epsilon_0^2$ .

On Fig. 2 is shown the energy dependence of the  $Y$ - $p$  cross sections evaluated with the GRV94 LO gluon distribution at scales  $\mu^2 = \epsilon_0^2$  (solid),  $2\epsilon_0^2$  (dashed), and  $4\epsilon_0^2$  (dotted). To bypass the question of the scale dependence of  $\epsilon_0$  we restricted our study to the massless target case and studied the cross section as a function of  $\lambda/\epsilon_0$ .

We first remark that the higher the scale  $\mu^2$ , the larger (respectively smaller) the cross section at high (respectively low) incident energy. At high energy ( $\lambda/\epsilon_0 \sim 10^4$ ) the uncertainty may be as high as a 100%. The situation is much better in the range  $\lambda/\epsilon_0 \sim 20$ –100 that is particularly relevant for

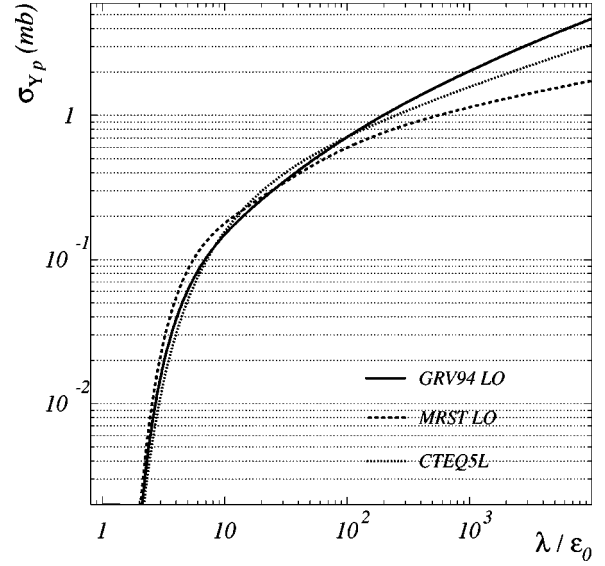


FIG. 3. Absolute  $\sigma_{Yp}$  cross section as a function of  $\lambda/\epsilon_0$  using GRV94 LO (solid), MRST98 LO (dashed), and CTEQ5L (dotted) gluon distribution. The scale has been fixed for all distributions to  $\mu^2 = 4\epsilon_0^2$ .

phenomenology. We also notice that the running of  $\alpha_S$  and that of  $G_p$  tends to somewhat compensate each other for the cross section at high energy.

We also investigated the consequences of changing the parameterization of the gluon distributions. Three leading order sets exist which may be evaluated at the scale  $\mu^2 = 4\epsilon_0^2$ . Figure 3 displays the energy dependence of the absolute cross section  $\sigma_{Yp}$  using GRV94 LO (solid), MRST98 LO (dashed) and CTEQ5L (dotted) gluon densities. The energy dependence proves to be rather independent of a specific choice for energies  $\lambda < 300\epsilon_0$ . At larger energies there is a rather strong dependence which leads to an uncertainty on the cross section comparable to that due to the scale variation (compare Figs. 2 and 3). The origin of this uncertainty is the poor knowledge of the gluon distribution at very low  $x$ .

## 2. Cross sections using GRV gluon distributions

We now turn to the discussion of the magnitude of the cross section. The  $J/\psi$  and  $Y$  cross sections are displayed on Fig. 4. They have been computed using the parameter set (i) with the GRV gluon density for the proton [16] and the pion [17] evaluated at  $\mu^2 = \epsilon_0^2$ .

These cross sections  $\sigma_{J/\psi h}$  (left) and  $\sigma_{Yh}$  (right) are found to strongly increase up to about 1 mb and 0.2 mb, respectively. The transition between low and high energy is situated around  $\sqrt{s_{J/\psi h}} = 8$  GeV and  $\sqrt{s_{Yh}} = 15$  GeV, respectively. We also notice that, depending on the set of parameters chosen [respectively (i) and (ii)], the ratio  $\sigma_{J/\psi h}/\sigma_{Yh}$  at high energy lies in the range 4–6, i.e., roughly the charm to bottom ratio of  $a_0^3\epsilon_0$ .

The energy dependence of  $\sigma_{\Phi\pi}$  turns out to be remarkably similar to the one in the proton channel, with a slightly smaller magnitude. This similarity is intimately related to the analogy that exists between the proton and the pion distribu-

<sup>8</sup>For consistency we use here and in the following the one-loop running coupling with  $n_f = 3$  and with the QCD scale determined by Refs. [16,17]:  $\Lambda^{(3)} = 232$  MeV.



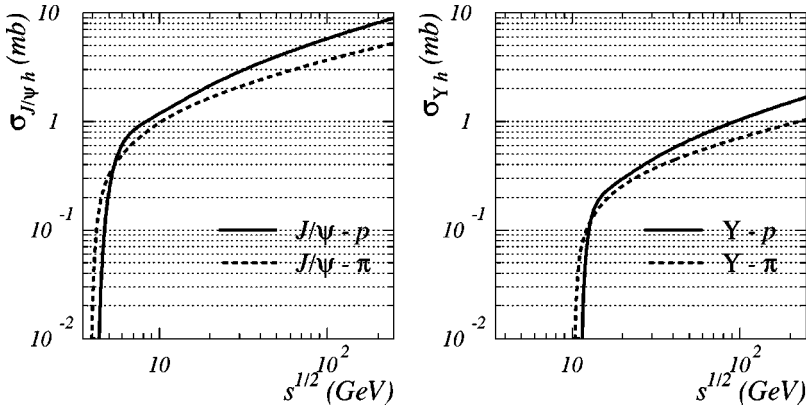


FIG. 4. Absolute cross sections  $\sigma_{\Phi h}$  as a function of the incident energy for  $J/\psi$  (left) and  $Y$  (right) with proton (solid), and  $\pi$  (dashed). The gluon distributions  $G_p(x)$  and  $G_\pi(x)$  used come from Ref. [16] and Ref. [17], respectively, evaluated at  $\mu^2 = \epsilon_0^2$ .

tions in the GRV approach. Needless to say that lacking small  $x$  experiments for the pion it has not been possible to verify this analogy so far. With GRV distributions and at high energy ( $\sqrt{s_{\Phi h}} = 200$  GeV) the ratio  $\sigma_{\Phi\pi}/\sigma_{\Phi p} \approx 0.6$ , independent of the quarkonium considered.

#### IV. CONCLUSION

The operator product expansion analysis has been widely used in the analysis of deep inelastic scattering. Subsequently, these very techniques proved useful to investigate heavy quark systems [3,4] allowing the calculation of the  $J/\psi$ - $p$  cross section within perturbative QCD. Such a cross section is of seminal importance in the context of heavy ion collisions.

The present study is a continuation of the work of Bhanot and Peskin and of a more recent paper by Kharzeev and collaborators [10]. Let us gather what have been carried out here.

First, the leading twist forward scattering amplitude has been given a simple integral expression, entailing a partonic representation for the total cross section. Such a description had been found in a different way in Ref. [4] in the case of massless targets.

Secondly, finite target mass corrections have been systematically incorporated. We showed that the cross section still assumes a partonic form though in terms of a modified energy variable. In addition to a shift of the reaction threshold, finite mass corrections add to the suppression of the cross section at low relative energy but become insignificant far above threshold. In the case of heavy targets, however, we noticed that the cross section becomes large just above (and even diverges at) threshold.

Last, the energy dependence of  $\sigma_{J/\psi h}$  and  $\sigma_{Y h}$  has been investigated for several targets. We found that  $\sigma_{\Phi\pi}$  and  $\sigma_{\Phi p}$  are strongly suppressed in the vicinity of the threshold. At large energy, the cross section is proportional to  $s^\delta$  for a target with  $G(x) \sim \text{const}/x^{1+\delta}$  at small  $x$ . With GRV gluon distributions this leads to slowly rising cross sections for both  $\Phi$ - $\pi$  and  $\Phi$ - $p$ . However, we should emphasize that the small- $x$  gluon distribution are not much constrained, especially that of the pion. Indeed the weak control we have on the gluon distribution, because of both the just mentioned poor small- $x$  knowledge and the sizeable scale dependence, turned out to be the main source of uncertainty in the present

approach. The  $\Phi'$  cross section have also been investigated, although the relevance of a perturbative approach is not fully satisfied for 2S states.

In addition to the hadron mass corrections considered here and beyond perturbative corrections, higher twist corrections may also lead to substantial modification for a not so heavy quark such as the charm. Indeed we noticed in Sec. II B that the threshold location may vary when one incorporates higher twist correction, making finite a cross section which is zero at leading twist. Considerations of this type of corrections is clearly outside the scope of the present study. Part of these corrections may be associated to the  $\Phi$  sector and in particular to the confining part of the heavy quark potential. Other corrections involving higher twist operators in the hadron target have presumably their counterparts in deep inelastic scattering.

As compared to the other approaches mentioned in the introduction the  $J/\psi$ - $\pi$  cross section is very tiny at  $\sqrt{s} = 4$  GeV. In the 4–7 GeV energy range it strongly increases driven by the intermediate  $x$  region in the gluon distribution. This  $x$  region is fairly under control thanks to the momentum sum rule and consequently the prediction, within the present approach, of cross section smaller than 1 mb below 7 GeV is rather robust.

A consequence of such a small cross section at small relative energies is that destruction of  $J/\psi$ 's by comovers become very unlikely. We are presently studying whether our results allows already for an answer to the question whether a quark gluon plasma is formed in ultra-relativistic heavy ion reactions. Our present approach is, however, limited to the  $J/\psi$  cross section, since for the excited states the binding energy is not large as compared to the confining scale.

#### APPENDIX A: SUM RULES FOR $\sigma_{\Phi h}$

In this first appendix, we establish the sum rules satisfied by the leading twist total cross section  $\sigma_{\Phi h}$ . This allows us to make contact with a similar derivation done in the case  $m_h = 0$  [4] and  $m_h \neq 0$  [10]. The starting point is the expression for the leading twist amplitude (12). Expressing  $M_n = d_n A_n$  and recalling that  $A_n$  is the  $n$ -th moment of the gluon density in the hadron target (see Sec. II A), we may write the series as

$$\begin{aligned}
 \mathcal{M}'(\lambda, m_h) &= a_0^3 \epsilon_0^2 \sum_{k' \geq 1} (\lambda/\epsilon_0)^{2k'} \int_0^1 \frac{dx}{x} x^{2k'} G(x) \\
 &\times \sum_{j \geq 0} \frac{(2k' + j)!}{j!(2k')!} d_{2k'+2j} \left( -\frac{m_h^2}{4\epsilon_0^2} x^2 \right)^j \\
 &+ a_0^3 \epsilon_0^2 \int_0^1 \frac{dx}{x} G(x) \sum_{j \geq 1} d_{2j} \left( -\frac{m_h^2}{4\epsilon_0^2} x^2 \right)^j.
 \end{aligned} \tag{A1}$$

Using the identities [14]

$$\begin{aligned}
 &\sum_{j \geq 0} \frac{(n+j)!}{j!n!} B\left(n+2j+\frac{5}{2}, \frac{5}{2}\right) z^j \\
 &= B\left(n+\frac{5}{2}, \frac{5}{2}\right) \\
 &\times {}_3F_2\left(\frac{5}{4}+\frac{n}{2}, \frac{7}{4}+\frac{n}{2}, 1+n; \frac{5}{2}+\frac{n}{2}, 3+\frac{n}{2}; z\right), \\
 &\sum_{j \geq 0} B\left(2j+\frac{9}{2}, \frac{5}{2}\right) z^j \\
 &= B\left(\frac{9}{2}, \frac{5}{2}\right) \times {}_3F_2\left(1, \frac{9}{4}, \frac{11}{4}; \frac{7}{2}, 4; z\right),
 \end{aligned}$$

the sums over  $j$  in Eq. (A1) leads to

$$\begin{aligned}
 \mathcal{M}'(\lambda, m_h) &= a_0^3 \epsilon_0^2 \sum_{k' \geq 1} d_{2k'} \tilde{A}(2k') (\lambda/\epsilon_0)^{2k'} \\
 &- a_0^3 \epsilon_0^2 \left( \frac{m_h^2}{4\epsilon_0^2} \right) d_2 \int_0^1 dx x G(x) \\
 &\times {}_3F_2\left(1, \frac{9}{4}, \frac{11}{4}; \frac{7}{2}, 4; -\frac{m_h^2}{4\epsilon_0^2} x^2\right), \tag{A2}
 \end{aligned}$$

where

$$\begin{aligned}
 \tilde{A}(n) &= \int_0^1 \frac{dx}{x} x^n G(x) \times {}_3F_2\left(\frac{5}{4}+\frac{n}{2}, \frac{7}{4}+\frac{n}{2}, 1+n; \frac{5}{2}+\frac{n}{2}, 3\right. \\
 &\left. + \frac{n}{2}; -\frac{m_h^2}{4\epsilon_0^2} x^2\right).
 \end{aligned}$$

We point out that Eq. (A2) is equivalent to the equation (15) of [10] with slightly different notations.

As noted in [4], performing the integral

$$\oint \frac{d\lambda}{2i\pi} \lambda^{-2l-1} \mathcal{M}'(\lambda, m_h)$$

around a counterclockwise contour enclosing the origin gives the coefficient of  $\lambda^{2l}$  in the amplitude (A2). Wrapping the contour around the  $u$  and  $s$  channel cuts, the contour at infinity giving no contribution,<sup>9</sup>

$$\frac{2}{\pi} \int_{m_h}^{+\infty} d\lambda \lambda^{-2l-1} \text{Im} \mathcal{M}'(\lambda, m_h) = a_0^3 \epsilon_0^2 d_{2l} \tilde{A}(2l) \epsilon_0^{-2l}.$$

We put  $m_h$  as a lower bound of the integral but this does not presume of the exact location of the threshold  $\lambda_0$  (necessarily greater than or equal to  $m_h$ ) implicitly contained in the set of sum rules (see below). Using the optical theorem one finally gets the sum rules for the  $\Phi$ - $h$  cross section

$$\int_{m_h}^{+\infty} d\lambda \lambda^{-2l-1} \sqrt{\lambda^2 - m_h^2} \sigma_{\Phi h}(\lambda) = \frac{\pi}{2} a_0^3 \epsilon_0^2 d_{2l} \tilde{A}(2l) \epsilon_0^{-2l}, \tag{A3}$$

which is what Bhanot and Peskin found [Eq. (3.10) in Ref. [4]] in the limit of massless target. In order to compare these results with [10], we introduce the variable  $y = m_h/\lambda$  to get

$$\int_0^1 dy y^{2l-2} \sqrt{1-y^2} \sigma_{\Phi h}(m_h/y) = \left( \frac{m_h}{\epsilon_0} \right)^{2l-1} I(2l) \tilde{A}(2l), \tag{A4}$$

with

$$I(n) = \frac{\pi}{2} a_0^3 \epsilon_0 d_n,$$

as introduced in [10]. The relation (A4) gives the set of sum rules that should replace that given by Eq. (16) of Ref. [10], where the prefactor  $(m_h/\epsilon_0)^{2l-1}$  is missing.

In order to verify that the sum-rule formalism leads to the same result as we obtained in the present study we need to solve Eq. (A4) for  $\sigma_{\Phi h}$ . This may be done using Laplace transform techniques. Equation (A4) writes

$$\int_0^1 dy y^{n-2} \sqrt{1-y^2} \sigma_{\Phi h}(m_h/y) = g(n), \quad n = 2, 4, \dots,$$

with

$$g(n) = \left( \frac{m_h}{\epsilon_0} \right)^{n-1} I(n) \tilde{A}(n).$$

Defining  $x = -\ln y$  and  $n' = n - 1$ , we get the relation

<sup>9</sup>Both the singularity pattern and asymptotic behavior of the scattering amplitude, which are necessary for the present construction to hold, are best studied within the approach of Sec. II. In Ref. [4], these properties were assumed from general properties of the elastic scattering amplitude.

$$\int_0^{+\infty} dx \exp(-n'x) \underbrace{\sqrt{1-\exp(-2x)} \sigma_{\Phi_h}(m_h \exp(x))}_{=f(x)}$$

$$=g(n'+1), \quad n'=1,3,\dots,$$

that is  $g(n'+1)$  is the Laplace transform of  $f(x)$ .

The above relation can be uniquely extended to a complex argument  $\nu$  (at least for  $\text{Re } \nu > \delta$ , see below) instead of the listed  $n'$ . We can then obtain  $f(x)$  by inverting the Laplace transform

$$f(x) = \frac{1}{2i\pi} \int_{\nu'_0-i\infty}^{\nu'_0+i\infty} d\nu \exp(\nu x) g(\nu+1), \quad (\text{A5})$$

where  $\nu'_0$  is an arbitrary real chosen so that the integration contour is located “at the right” of all singularities of  $g(\nu+1)$ . For gluon distribution behaving as  $x^{-(1+\delta)}$  for  $x \rightarrow 0$ , integrals of the type  $\int_0^1 dx x^\nu G(x) {}_3F_2$  are well behaved provided  $\text{Re } \nu > \delta$ . As a consequence we performed the inverse Laplace transform choosing  $\nu'_0 > \delta$ .

Setting  $\nu = \nu'_0 + iu = \nu_0 - 1 + iu$ , and then  $\lambda = m_h \exp(x)$ , we thus obtain

$$\begin{aligned} & \sqrt{1-\exp(-2x)} \sigma_{\Phi_h}(m_h \exp(x)) \\ &= \frac{1}{2\pi} \int_{-\infty}^{+\infty} du \exp[(\nu_0-1+iu)x] g(\nu_0+iu), \end{aligned}$$

and then

$$\begin{aligned} \sigma_{\Phi_h}(\lambda) &= \frac{\lambda}{2\pi\sqrt{\lambda^2-m_h^2}} \int_{-\infty}^{+\infty} du \left(\frac{\lambda}{m_h}\right)^{\nu_0-1+iu} g(\nu_0+iu) \\ &= \frac{\lambda}{2\pi\sqrt{\lambda^2-m_h^2}} \int_{-\infty}^{+\infty} du \left(\frac{\lambda}{\epsilon_0}\right)^{\nu_0-1+iu} \\ & I(\nu_0+iu) \tilde{A}(\nu_0+iu), \end{aligned} \quad (\text{A6})$$

for every  $\nu_0 > 1 + \delta$ . Let us remark that the  $\epsilon_0$  energy scale appearing in the first factor of the integrand would be  $m_h$  with the sum rules proposed in [10]. The difference between these two results is important when one considers the  $m_h \rightarrow 0$  limit, in which case the latter expression is ill-defined contrarily to ours, given in Eq. (A6).

We carried out a numerical evaluation and found out that it reproduces the results obtained in the main body of the paper. One critical point in the comparison between the two approaches is the verification that the threshold is located at the predicted value, that is, in particular, that the numerical

result is compatible with zero below this threshold [a point which is far from evident when one looks at Eqs. (A6) or (A3)].

## APPENDIX B: 2S STATES

In this appendix, calculations of the  $\Phi$  cross sections are extended to the 2S states  $\Phi'$ . The modification amounts to replacing the 1S coefficients  $d_n^{(1S)}$  (denoted  $d_n$  so far) by the 2S coefficients [3]

$$d_n^{(2S)} = \frac{16^3}{3N_c^2} \frac{\Gamma(n+5/2)\Gamma(5/2)}{\Gamma(n+7)} (16n^2+56n+75).$$

Expressing  $d_n^{(2S)}$  as a function of the 1S coefficients

$$d_n^{(2S)} = 4^n (4d_n^{(1S)} - 24d_{n+1}^{(1S)} + 36d_{n+2}^{(1S)}),$$

allows one to get an integral representation for the 2S coefficients

$$d_n^{(2S)} = 4^n \int_0^1 \frac{dx}{x} x^n f^{(2S)}(x), \quad (\text{B1})$$

with

$$f^{(2S)}(x) = \frac{16^3}{3N_c^2} x^{5/2} (1-x)^{3/2} (2-6x)^2,$$

which is the ingredient needed to carry out the procedure outlined in Sec. II. The changes are that the function  $h$  has to be replaced by  $h^{(2S)} = G \otimes f^{(2S)}$  and that it is now evaluated at  $\epsilon/\lambda$ ,  $\epsilon/\lambda_+$ , or  $\epsilon/\lambda_-$  instead of  $\epsilon_0/\lambda$ ,  $\epsilon_0/\lambda_+$ , or  $\epsilon_0/\lambda_-$  where  $\epsilon = \epsilon_0/4$  is the binding energy of the 2S state. The partonic expression is thus similar with

$$\sigma_{\Phi'g}(\omega) = 16 \frac{16^3 \pi}{6N_c^2} a_0^3 \epsilon_0 \frac{(\omega/\epsilon-1)^{3/2} (\omega/\epsilon-3)^2}{(\omega/\epsilon)^7} \theta(\omega-\epsilon).$$

The energy dependence  $\sigma_{\Psi'p}(s)$  has been computed using the parameter set (i). The cross section diverges at threshold ( $\sqrt{s} \approx 11$  GeV) and decreases to a minimum of about 4 mb at a center of mass energy 0.6 GeV above threshold. Then the cross section increases smoothly [ $\sigma_{\Psi'p}(s) \propto s^\delta$ ] and reaches 30 mb by  $\sqrt{s} \approx 200$  GeV. We notice that at high energy the ratio  $\sigma_{\Phi'h}/\sigma_{\Phi_h} \approx 20$  for all incident hadrons. Since  $r(2S) = \sqrt{10} r(1S)$ , this result lies somewhat above the geometrical expectation  $r^2(2S)/r^2(1S)$ .

We have already insisted on the fact that the LT perturbative analysis is most likely not adequate to describe the  $\psi'$  channel. In this case, the cross section amounts to  $\sigma_{\Psi'p}(\sqrt{s}) = 30$  mb at  $\sqrt{s} = 10$  GeV.

[1] T. Matsui and H. Satz, Phys. Lett. B **178**, 416 (1986).

[2] Fermilab E866/NuSea Collaboration, M.J. Leitch *et al.*, Phys. Rev. Lett. **84**, 3256 (2000).

[3] M.E. Peskin, Nucl. Phys. **B156**, 356 (1979).

[4] G. Bhanot and M.E. Peskin, Nucl. Phys. **B156**, 391 (1979).

[5] K. Martins, D. Blaschke, and E. Quack, Phys. Rev. C **51**, 2723 (1995).

[6] C.-Y. Wong, E.S. Swanson, and T. Barnes, Phys. Rev. C **62**,

- 045201 (2000).
- [7] S.G. Matinyan and B. Müller, Phys. Rev. C **58**, 2994 (1998).
- [8] K. Haglin, Phys. Rev. C **61**, 031902 (2000).
- [9] Z. Lin and C.M. Ko, Phys. Rev. C **62**, 034903 (2000).
- [10] D. Kharzeev, H. Satz, A. Syamtomov, and G. Zinovjev, Phys. Lett. B **389**, 595 (1996).
- [11] H. Georgi and H.D. Politzer, Phys. Rev. D **14**, 1829 (1976).
- [12] O. Nachtmann, Nucl. Phys. **B63**, 237 (1973); **B78**, 455 (1974).
- [13] G. Serman *et al.*, Rev. Mod. Phys. **67**, 157 (1995).
- [14] M. Abramowitz and I. Stegun, *Handbook of Mathematical Functions* (Dover, New York, 1972).
- [15] A. De Rújula, H. Georgi, and H.D. Politzer, Ann. Phys. (N.Y.) **103**, 315 (1977).
- [16] M. Glück, E. Reya, and A. Vogt, Z. Phys. C **67**, 433 (1995).
- [17] M. Glück, E. Reya, and A. Vogt, Z. Phys. C **53**, 651 (1992).
- [18] M. Glück, E. Reya, and A. Vogt, Eur. Phys. J. C **5**, 461 (1998).
- [19] A.D. Martin, R.G. Roberts, W.J. Stirling, and R.S. Thorne, Eur. Phys. J. C **4**, 463 (1998); Phys. Lett. B **443**, 301 (1998).
- [20] H.L. Lai *et al.*, Eur. Phys. J. C **12**, 375 (2000).